Research Paper

PAIN®

VIDEO

Ocular nociception and neuropathic pain initiated by blue light stress in C57BL/6J mice

Nan Gao[a,*], Patrick S.Y. Lee[a], Jitao Zhang[b], Fu-shin X. Yu[a]

Abstract

To elucidate the physiological, cellular, and molecular mechanisms responsible for initiating and sustaining ocular neuropathic pain, we created a blue light exposure model in C57BL/6 mice. Mice were exposed to 12 hours of blue or white light followed by 12 hours of darkness. Before blue light exposure, baseline tear secretion, stability, and ocular hyperalgesia were assessed by measuring hyperosmotic or hypoosmotic solution-induced eye wiping, wind-induced eye closing, and cold-induced eye blinking. At 1 day after blue light exposure, alterations in hypotonic or hypertonic-induced eye wiping and tear film abnormalities were observed. Eye-wiping behaviors were abolished by topical anesthesia. The cold-stimulated eye blinking and wind-stimulated eye closing behaviors began after day 3 and their frequency further increased after day 9. Blue light exposure reduced the density of nerve endings and increased their tortuosity, the number of beadlike structures, and the branching of stromal nerve fibers, as assessed by whole-mount confocal microscopy. Blue light exposure also increased TRPV1, but not TRPV4 staining intensity of corneal-projecting neurons in the trigeminal ganglia, as detected by FluoroGold retrograde labeling and immunohistochemistry. TRPV1 and substance P expression was increased, whereas CGRP expression deceased at the mRNA level in isolated corneal projecting neurons. Hence, our blue light exposure B6 mouse model for assessing tearing and ocular hyperalgesia is useful for studying ocular pain and its underlying mechanisms. Blue light–induced alterations in tearing and ocular hyperalgesia may be related to the elevated expression of TRPV1, substance P, or the suppressed expression of CGRP at the ocular surface.

Keywords: Ocular neuropathic pain, Blue light, Computer vision syndrome, Hyperalgesia

1. Introduction

The cornea is innervated by sensory nerves from the ophthalmic branch of the trigeminal ganglia.[22] It has the highest density of sensory nerve endings in the body and is highly sensitive to noxious stimuli.[6] When the pain is initiated or sustained by dysfunctional elements in the nociceptive system, it is known as neuropathic pain.[12] Corneal nociceptors are predominantly unmyelinated C fibers, with the remainder being the lightly myelinated Aδ fibers.[22,49] As with pain fibers elsewhere in the body, corneal nerve endings have various receptors, including the transient receptor potential channels TRPV1, TRPV4, TRPA1, as well as TRPM8.[1,25,48] These receptors can respond to osmotic, mechanical, thermal, and chemical stimuli.[49] TRPV1 nerves were accounted for a higher proportion of corneal nerves at the ocular surface.[1,26] Despite its insensitivity to cold, TRPV1 has been shown to sensitize TRPM8$^+$ sensory neurons and promote neuropeptide substance P (SP) release to signal cold nociception.[29] TRPV4 is responsible for sensing hypoosmotic and mechanical signals.[21] Neural TRPV4 has been shown to be critical to maintaining stemness of peripheral or limbal basal cells.[46] Compared with TRPV1, the role of TRPV4 in neuropathic pain is less clear. The involvement of these nociceptors in mediating corneal response to noxious stimuli and in ocular surface sensitization and hyperalgesia are largely elusive, partially due to the lack of proper animal models that resemble the pathogenesis of human ocular neuropathic pain.

Existing ocular pain models, including humidity chambers, topical agents, cauterization, finasteride, alkali burns, and lacrimal gland excision, are used mainly for the study of dry eye disease or short-lived acute pain behaviors.[4,8,10,18,31,54,63,64] Computer vision syndrome encompasses a range of ocular and visual symptoms, including tearing, gritty, dryness, redness, burning sensation, and ocular pain associated with screen use.[32,44,50] The major culprit behind computer vision syndrome is believed to be blue light.[9] Blue light is a high-energy and high-frequency light; prolonged exposure can result in photophobia, ocular pain, cataract, and age-related macular degeneration.[3,30,36,45,53,56] Using a B6 mouse blue light exposure model, strong (mice housed in mirrored-wall boxes) and acute (3 hours blue light exposure has been shown to increase corneal mechanical sensitivity, tear secretion, and photophobia, immediately after illumination or within 3 days of recovery).[36] Hence, blue light exposure may be used as a pathogenic factor for establishing an animal model of ocular neuropathic pain.

We established a mouse model of ocular neuropathic pain or computer vision syndrome, with mice reared in alternating cycles of 12 hours blue light and 12 hours of darkness. We also

Sponsorships or competing interests that may be relevant to content are disclosed at the end of this article.

[a] *Department of Ophthalmology, Visual and Anatomical Sciences, Wayne State University School of Medicine, Detroit, MI, United States,* [b] *Biomedical Engineering Department, Wayne State University, Integrative Biosciences Center, Detroit, MI, United States*

**Corresponding author. Address: Kresge Eye Institute, Wayne State University School of Medicine, 4717 St. Antoine Blvd, Detroit, MI 48201, United States. Tel.: +1 3135776461. E-mail address: ec0422@wayne.edu (N. Gao).*

Supplemental digital content is available for this article. Direct URL citations appear in the printed text and are provided in the HTML and PDF versions of this article on the journal's Web site (www.painjournalonline.com).

PAIN 00 (2023) 1–11

http://dx.doi.org/10.1097/j.pain.0000000000002896

developed several behavior-based assessments of ocular pain. Our study revealed that blue light exposure enhanced osmotic-induced eye wiping, cold-induced eye blinking, and wind-induced eye closing at different time points, compared with controls. These abnormalities were associated with sensory neuron degeneration or malfunction.

2. Methods

2.1. Animals

Wild-type C57BL/6 (B6) mice (8 weeks of age; 20-24 g weight; male and female) were purchased from The Jackson Laboratory (Bar Harbor, ME). The animals were treated in compliance with the ARVO Statement for the Use of Animals in Ophthalmic and Vision Research. The Institutional Animal Care and Use Committee of Wayne State University approved all animal procedures.

2.2. Blue light exposure model of ocular neuropathic pain

Ten (5 males and 5 females) 8-week-old C57BL/6 mice from Jackson Laboratory were reared in cycles consisting of 12 hours neutral white or blue light (420 nm wavelength), alternating with 12 hours darkness (WL/BL:D). The light source is an overhead 15-W light bulb (Babaoshop) placed 20 cm above the mice. The irradiance of blue light was measured with a power meter (model: PM120D) at the center (area A) and 4 sides (total area − area A) of the cage. The average irradiance was 2.722 mW/cm^2 (vs 6 mW/cm^2 for Marek et al.[36]). The radiant exposure was 117.6 J/cm^2 (versus 64.8 for Marek et al.), and average illuminance was 320 Lux (vs 400 for Marek et al). There were no other sources of ambient lighting. Mice underwent the first white or blue light cycle starting at 6 AM and then a night cycle at 6 PM Behavioral tests were performed at 10 AM the following morning; this was considered as "1 day postexposure (p.e.)" (the extra 4 hours of light exposure are to overcome the effects of potential dark recovery). This WL/BL:D cycle and testing scheme apply to all other time points. For example, 7 day p.e. was a full 7 exposures of WL/BL:D plus 4 hours light exposure on day 8 (the day of measurement). White light and blue light–exposed eyes were also treated with 1 drop of topical proparacaine; 5 minutes after the treatment, the eyes were stimulated with 1 M NaCl, and the number of eye-wiping behaviors was counted. Tearing and behavior tests (described below) were performed for up to 14 days.

2.3. Aqueous tear production and Rose Bengal staining

Tear production was measured with phenol red–impregnated cotton threads (ZONE-QUICK, Billerica, CA).[62] The threads were held with jeweler forceps and applied to the lateral canthus for 5 seconds. The length of wetting of the thread was measured in millimeters.

The corneal surface was examined with 1% Rose Bengal staining and photographed under a slit lamp. To quantitate Rose Bengal staining, each cornea was divided into 4 quadrants, and each quadrant was scored based on the following scale: 0, no staining; 1, punctate staining; 2, continuous staining covering <50% area; 3, continuous staining covering ≥50% area but not confluent; and 4, confluent staining covering ≥90%. The final score for each cornea is the sum of the scores from all quadrants.[62]

2.4. Behavior tests

A: Eye-wiping test. The eye-wiping test was performed as previously described.[16,55] The mice were placed in a glass testing chamber to allow habituation for 30 minutes. Test solutions of 5 μL 1 M NaCl or H_2O were applied to the center of the corneas. The number of "eye-wiping" behaviors using the forelimbs was recorded on video and counted over 90 seconds. *B: Wind stimulation.* A variable area flow meter (Western Medica) was connected with an airflow source by a polyvinyl chloride (PVC) tube with a 10 μL pipette tip at the end. Wind stimulation was applied using airflow of 2 L/minute at room temperature (23°C). During testing, mice were restrained manually, and their eyes were placed 5 mm away from the airflow. The "eye-closing" behaviors were photographed and video recorded. The maximum ocular length or width ratio was calculated based on the measurement of the length and width of the palpebral fissure.[23] Moreover, "eye-closing" behaviors are defined as holding the eyelids closed without blinking, in contrast to blinking being less than or equal to 1 to 2 seconds. Tightening and closing of the eyelids were considered surrogate measure of pain.[24,29] *C: Cold stimulation.* Cold stimulation was applied using temperature-controlled airflow.[29] Like wind stimulation, a variable airflow meter was connected with an airflow source by a PVC tube with a 10 μL pipette tip at the end. To control temperature, the PVC tube was immersed in a water bath, and the tip at the end of PVC was kept out of the water bath to avoid water entering, and the temperature was adjusted until the outflow air was maintained at 12°C. A low flow speed of 0.5 L/minute was used. The number of blinks was recorded on video and counted over 30 seconds. Corneal sensitivity was measured using Cochet–Bonnet contact esthesiometer.[65]

2.5. Corneal whole-mount confocal microscopy

At the end of the tearing and behavioral tests (day 15), 4 corneas (2 from male and 2 from female mice) were subjected to whole-mount confocal microscopy (WMCM) to assess for anatomical changes in corneal innervation. Because no gender differences were observed in tearing, behavior tests, and corneal sensory innervation at day 14, in the following experiments, female mice only were subjected to the indicated exposure cycles. Three tissues per group were processed for WMCM (7 days postexposure) and immunostaining of SP (3 and 5 days post exposure), as well as retrograde labeling for immunohistochemistry and quantitative polymerase chain reaction (qPCR).

Whole-mount confocal microscopy was used for β-tubulin III (a panneuronal marker) and SP staining. Corneas were excised and fixed in 4% paraformaldehyde (Electron Microscopy Sciences, Hatfield, PA) and stored at 4°C until further processing. Whole-mount staining of anti–β-tubulin III (R&D System, Minneapolis, MN) or anti-SP (Sigma, St. Louis, MO) was performed as previously described.[19] Corneal whole mounts were examined using a Nikon ECLIPSE 90i microscope. Corneal innervation was quantified as the percentage of threshold area positive for β-tubulin III staining with ImageJ software. The number of branch points on the main nerve fibers (per mm^2), nerve tortuosity (showing abrupt and frequent changes in direction, defined as the number of acutely angled fibers per mm^2),[42] and the number of beadlike formations (per mm^2) were manually counted and verified by a second blinded laboratory member.

2.6. Trigeminal ganglion immunohistochemistry

To label trigeminal ganglia corneal-projecting neurons, 0.5 μL of 4% FluoroGold (FG, Biotium, Fremont, CA) or 5 mg/mL wheat germ agglutinin-Alexa Fluor 555 (WGA, Thermo Fisher Scientific, Waltham, MA) in phosphate buffered saline (PBS) was injected into the corneal stroma with Nanofil syringe.[28] Mice were euthanized for trigeminal ganglia immunohistochemistry staining or cell sorting 3 days after injection.

FluoroGold-labeled trigeminal ganglia were fixed in 10% formaldehyde for 4 hours, embedded in Tissue-Tek optimum cutting

temperature (OCT) compound (Sakura Finetek, Torrance, CA), and frozen in liquid nitrogen. Next, 6-μm thick sections were cut and mounted to polylysine-coated glass slides. Slides were blocked with 10 -mM sodium phosphate buffer containing 2% Bovine serum albumin (BSA) for 1 hour at room temperature. Sections were then incubated with mouse anti-TRPV1, anti-TRPV4 (Alomone Labs, Cheshire, WA), or anti-SP (Millipore Sigma, St. Louis, MO). This was followed by a secondary antibody, Fluorescein isothiocyanate (FITC)-conjugated goat anti-hamster and cy3-conjugated anti-rabbit IgG (Jackson ImmunoResearch Laboratories, West Grove, PA), and slides were mounted with Vectashield mounting medium and examined under confocal microscopy. Controls were similarly treated, but the primary antibodies were replaced with nonspecific IgG.

2.7. Enrichment of corneal-projecting neurons

Two days post-Alexa Fluor 555 WGA labeling, the mice were exposed to BL:D/WL:D cycles. After 1 day, B6 mice were anesthetized; trigeminal ganglia were removed and cut into small pieces, followed by enzymatic dissociation using 60 U/mL papain, 4 mg/mL collagenase II, and 4.7 mg/mL dispase. Neurons were isolated by Percoll density–gradient centrifugation as previously described.[35] Neurons were labeled by Sytox (dead cell stain, eBioscience, Waltham, MA) for assessing viability. The labeled neurons were sorted by NanoCellect and collected as corneal-projecting neurons (WGA^+ $Sytox^-$) and noncorneal-projecting neurons (WGA^- $Sytox^-$). The collected neurons were subjected to qPCR analysis.

2.8. Real-time PCR

cDNA was generated from the sorted corneal-projecting neurons (CPNs) and non-$CPNs^-$. cDNA using Invitrogen SuperScript III Cells Direct cDNA Synthesis Kit (Millipore Sigma, St. Louis, MO), according to the manufacturer's recommended protocol, followed by analysis using real-time PCR with Power SYBR Green PCR Master Mix (Applied Biosystems, Waltham, MA), based on β-actin levels. Primer sequences were as follows: TRPV1, TGCCAGAGTATGCCCAGAGC and GGCTGGGGGCTCAGATTCAT; CGRP, AGCACTGCTCAACTATGA and AGGTGATGGCGTTCAAGTTCT; galanin, ATGCCATTGACAACCACAGA and GGTCTCCTTTCCTCCACCTC; Tac1, GGCCAAGGAGAGCAAAGA and CGAGGATTTTCATGTTCGATT; TRPV4, GCTCCCAGAAAGCACAGTTC and AGATGTGGCTAACCGTGTCC; CNTFRa, CACAACACTACGGCCATCAC and GGTAGCGCAGGAAGAACTTG; NGFR, TTGCTTGCTGTTGGAATGAG and AAATACCACCGAGCACAAGG; and TAFA4, AGGGACAT TCACGGTCACTC and CAGCACCCACTTAGCACAGA.

2.9. Statistical analyses

Data were presented as the mean ± SD. Experiments with a single treatment group was analyzed for statistical significance using a Student *t* test. Experiments with more than 2 groups were analyzed using 1-way analysis of variance (ANOVA), and if more than 2 sets of groups of mice were used, a 2-way ANOVA was used. Analysis of variance analysis was followed by the Tukey post hoc test. Significance will be accepted at $P < 0.05$.

3. Results

3.1. Blue light exposure increased hyperalgesia in B6 mice

We first investigated whether blue light exposure induces ocular neuropathic pain in B6 mice. Mice were exposed to alternating cycles of 12 hours blue light/12 hours darkness, with 12 hours white light/12 hours darkness cycles as the control. We observed that blue light exposure increased hypertonic or hypotonic solution–induced eye-wiping behaviors within a 90 seconds window compared with control mice or baseline measurements before blue light exposure. This alteration was observed starting after day 1 of exposure. It remained elevated levels at 14 days after exposure (p.e.) without significant upregulation or down-regulation (**Figs. 1A and B**). Treating the blue light and white light–exposed mice with proparacaine eye drops greatly reduced the number of hyperosmolarity-induced eye-wiping behaviors and abolished blue light–induced hyperalgesia (**Fig. 1C**).

Ocular hyperalgesia may be provoked by noxious stimuli such as cold, strong wind, and bright sunlight in patients.[14] Hence, we investigated behavioral changes in blue light–exposed mice in response to wind and cold stimulation. In our model, wind-induced eye-closing behaviors were tested by an airflow system connected with a PVC tube (**Fig. 2A**) and quantified as the ratio of the length and width of the palpebral fissure[39] (**Fig. 2B**; Video 1, and Video 2) while cold-induced eye-blinking behaviors within a 90 seconds window were counted. Unlike hypertonic or hypotonic solution–induced eye-wiping, wind-induced eye-closing, and cold-induced eye-blinking behaviors were increased starting from 3 days p.e. and further increased at 7 days p.e. and reached a peak at 9 days p.e. (**Figs. 2C and D**).

3.2. Blue light exposure impaired tear film integrity and increased tear deficiency

Dry eye disease is one of the most common symptoms associated with computer vision syndrome and ocular neuropathic pain.[50,51] To determine whether dry eye disease accompanies hyperalgesia in our model, blue light–exposed mice were examined with fluorescein and Rose Bengal staining, as well as Schirmer testing. Blue light–exposed mice showed increased Rose Bengal staining (expressed as staining scores reflecting stained surface area, with 0 as no staining and 12 as 100% staining), compared with control mice as early as 1 day p.e (4.20 ± 0.89 vs 0.60 ± 0.54) (**Figs. 3A and B**). No fluorescein staining was observed (data not shown). Meanwhile, blue light exposure reduces tear secretion, starting from 1 day p.e. compared with the white light–exposed mice (3.58 ± 1.21 mm vs 5.20 ± 1.30 mm), and tear secretion continued to decline after 7 days (1.90 ± 0.74 mm) (**Fig. 3C**).

3.3. Blue light exposure impairs corneal innervation and increases nerve sprouting

Ocular neuropathic pain is associated with malformed corneal sensory fibers and endings, namely, microneuromas, which are commonly seen in patients with neuropathic corneal pain.[43] To determine if blue light exposure is causative for these sensory fiber abnormalities, corneas were stained for β-tubulin III (pan-neuronal marker) and examined using whole-mount confocal microscopy at 7 and 14 days after exposure (p.e.) (**Fig. 4A**). At the central cornea, the densities of sensory nerve fibers and endings were 19.9% ± 1.77% vs 14.70% ± 0.42% at 7 days p.e. and 18.34% ± 0.66% vs 12.47% ± 0.18% at 14 days p.e. in white light vs blue light–exposed corneas, respectively (**Fig. 4B**). The abnormalities of corneal sensory nerves were also quantitated by counting the number of branches, tortuous (acutely angled fibers per mm^2), and beadlike fibers or endings. Blue light exposure increased branching of the major nerve fibers: There were 6 ± 0.95 (7 days p.e.) and 6 ± 0.5 (14 days p.e.) branches in white light–exposed corneas vs 6 ± 0.6 (7 days p.e) and 9 ± 0.8 (14 days p.e.) branches in blue light–exposed corneas (**Fig. 4C**). Blue

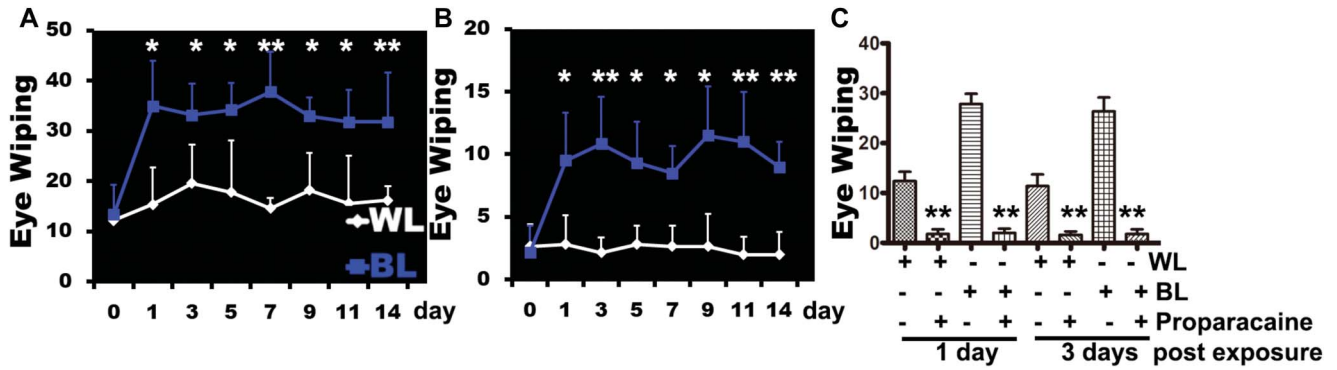

Figure 1. Effects of hyper or hypoosmotic-induced hyperalgesia on blue light–exposed mice. B6 mice were reared in cycles of either white (WL) or blue light (BL) alternating with darkness for 1 to 14 days. They were then placed in a glass testing chamber and allowed to habituate for 30 minutes. Five microliter of 1M NaCl (hypertonic stimulus) (A) or H_2O (hypotonic stimulus) (B) was applied to the ocular surface. (C) Topical proparacaine was applied to the cornea for 5 minutes, and 1M NaCl was then applied to the ocular surface. The activity was recorded on video. Number of eye-wiping behaviors within 90 seconds were counted (the mean of the number of eye-wiping behaviors was calculated and shown by y-axis; the days after exposure to light were indicated by x-axis). (*$P < 0.05$, **$P < 0.01$, n = 10, 5 male and 5 female). Data represent a representative experiment (from 2 independent experiments) performed in a single run. Experimental data were not pooled because the measurements showed some variations among 2 experiments.

light exposure increased nerve tortuosity (arrows, **Fig. 4D**), with 25 ± 9.29 tortuous fibers at 7 days p.e. and 26 ± 4.24 tortuous fibers at 14 days p.e. in white light–exposed corneas, vs 58 ± 4.97 tortuous fibers at 7 days p.e. and 46 ± 7.53 tortuous fibers at 14 days p.e. in blue light–exposed corneas. Moreover, blue light also increased the number of beadlike formations (arrowheads, **Fig. 4E**): There were 34 ± 11.11 (7 days p.e) and 43 ± 6.58 (14 days p.e) formations in white light–exposed corneas and 180 ± 53.17(7 days p.e) and 203 ± 37.94 (14 days p.e) formations in blue light–exposed corneas.

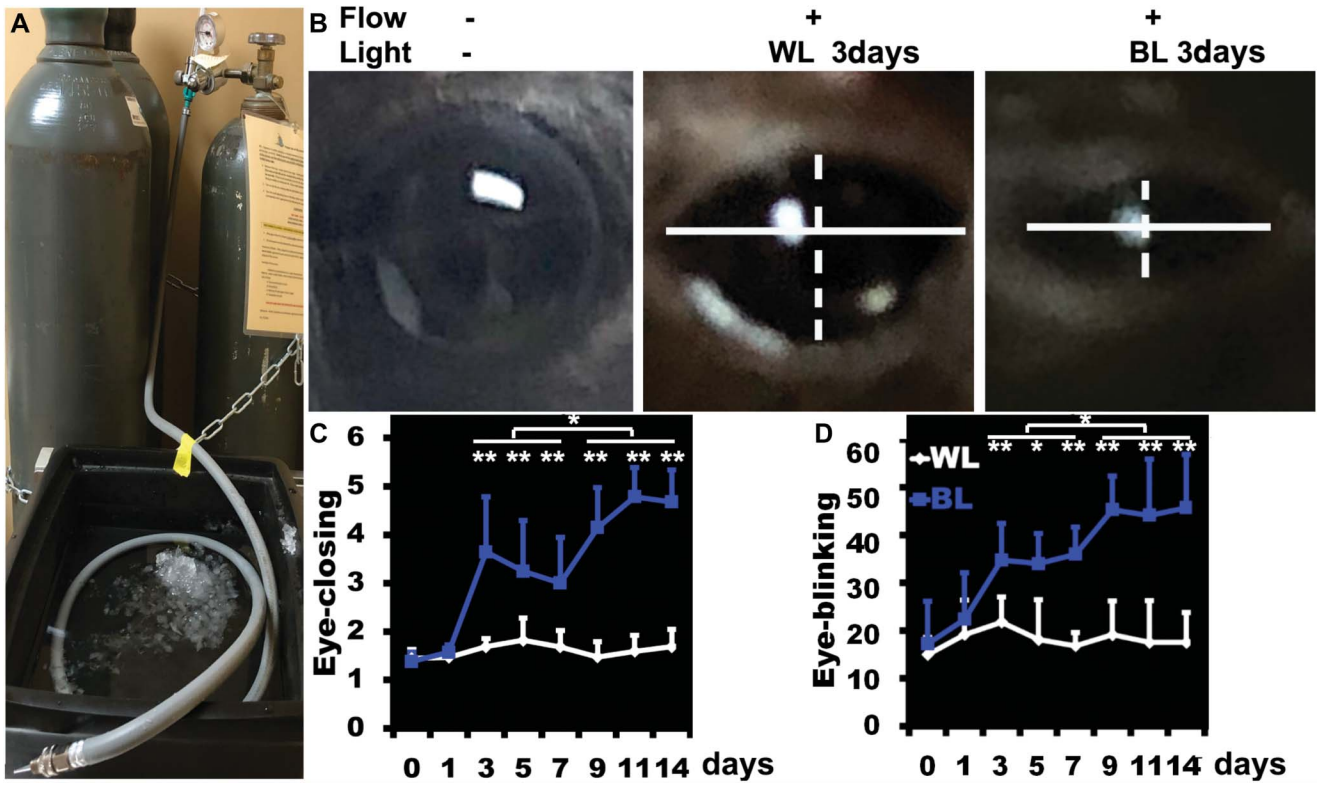

Figure 2. Wind-stimulated and cold-stimulated ocular hyperalgesia in blue light–exposed mice. Mice were reared in a prespecified number of cycles of either white or blue light alternating with darkness at the indicated times. A variable airflow meter was connected with an airflow source by a PVC tube with a 10 μL pipette tip at the end. To control temperature, the PVC tube was immersed in a water bath, and the tip at the end of PVC was kept out of the water bath to avoid water entering, and the temperature was adjusted until the outflow air was maintained at 12°C. A low flow speed of 0.5 L/minute was used (A). Eye-closing responses were photographed under wind stimulation. Wind stimulation was applied using airflow of 2 L/minute at room temperature (23°C) (B). Solid and dashed lines indicate the length and width of the palpebral fissure, respectively. The representative length or width ratio changes of white and blue light–exposed mice in response to wind at the indicated times (C). The representative eye blinking of white light (WL) and blue light (BL)-exposed mice in response to cold air (12°C) (D) (the mean of length or width ratio or the number of eye blinking was calculated and shown by y-axis; the days after exposure to light were indicated by x-axis) (*$P < 0.05$, **$P < 0.01$, n = 10, 5 male and 5 female).

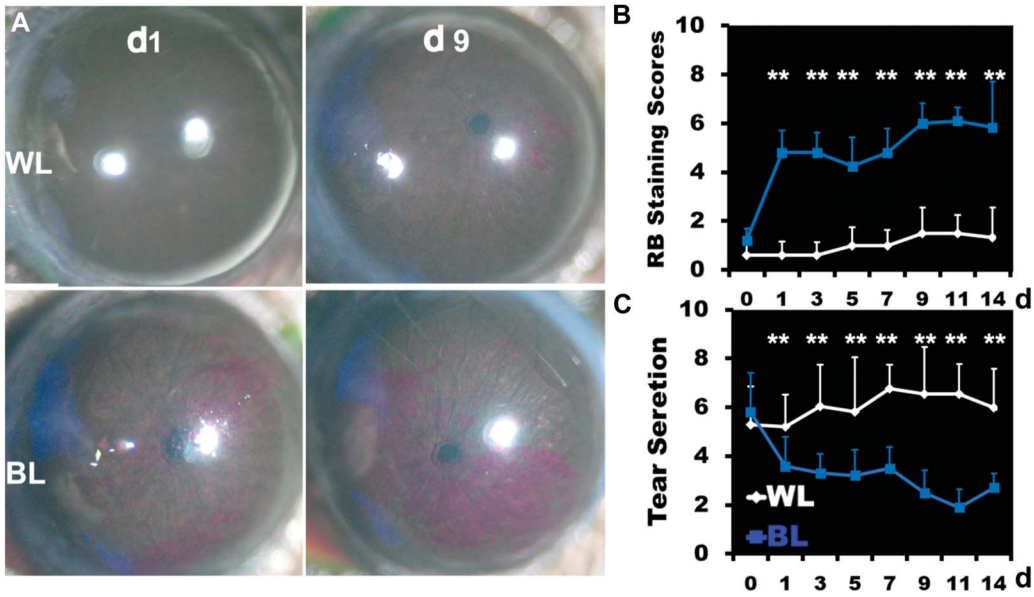

Figure 3. Effects of tear secretion in blue light–exposed mice. The mice were reared in cycles of either white (WL) or blue light (BL) alternating with darkness for 14 days (C). Corneas were stained with 1% RB and photographed (A). Rose Bengal staining scores were assessed (B). Tear secretion was measured by applying phenol red–impregnated cotton threads to the ocular surface for 60 seconds, and wetting of the thread was measured in millimeters using the scale on the cotton thread (C). The mean of scores or the length of the wetting thread was calculated and shown by y-axis; the days of exposure to light were indicated by x-axis (**$P < 0.01$, n = 10, 5 male and 5 female).

Consistent with these anatomical changes, the sensitivity of blue light–exposed corneas, as measured with the Cochet–Bonnet anesthesiometer, was significantly lower than that of white light–exposed control eyes at 7 and 14 days p.e. (**Fig. 4F**).

3.4. Blue light exposure enhances TRPV1 expression in the trigeminal ganglia

To further understand the mechanism underlying blue light–induced hyperalgesia, we next examined the expression of transient receptor potential (TRP) channels in the trigeminal ganglia. As corneal sensory nerves make up only a small fraction of neurons in the trigeminal ganglia, identifying these cells is essential for accurately determining the expression or activation of genes in response to blue light exposure. Hence, we injected FluoroGold into the corneal stroma to serve as a retrograde neuronal tracer. In FluoroGold-injected corneas, only β-tubulin III$^+$ neuronal fibers were labeled by FluoroGold (Supplementary materials 2, available as supplemental digital content at http://links.lww.com/PAIN/B805). As expected, retrograde-labeled corneal-projecting neurons were located in the dorsomedial part of the ophthalmic (V1) division, away from the maxillary (V2) and mandibular (V3) region of the trigeminal ganglia (**Fig. 5A**).[41] In white light–exposed mice, most but not all FluoroGold-labeled corneal-projecting neurons are also TRPV1$^+$ in the labeled region of the trigeminal ganglia, and the TRPV1$^-$ corneal-projecting neurons (^) are likely Aδ or nonpeptidergic C fibers. TRPV4 staining, on the other hand, in most cases, overlapped with only a portion of FluoroGold-stained corneal-projecting neurons. In blue light–exposed mice, these TRPV1$^+$ neurons showed increased staining intensity, indicative of increased expression. Many TRPV1^{high} neurons are also TRPV4$^+$ (arrows). There are, however, TRPV1$^+$ FluoroGold$^+$ TRPV4$^-$ (*) and TRPV1$^+$ TRPV4$^-$ FluoroGold$^-$ neurons (arrowhead, indicative of noncorneal-projecting neurons) (**Fig. 5B**).

3.5. Blue light exposure upregulates TRP channel and neuropeptide expressions at the mRNA levels in the corneal-projecting neurons

To understand the mechanism underlying TRPV1/4-mediated ocular nociception, we investigated the involvement of neuropeptides and neurotrophic factor receptors in the sensitization of ocular nociception. To that end, we labeled corneal-projecting neurons using stromal injection of WGA, followed by the viability assessment (Sytox$^-$ staining) (**Fig. 6A**) and sorting (NanoCellect Wolf Cell Sorter), resulting in enriched WGA$^+$ (ie, corneal-projecting neurons) and WGA$^-$ neurons (noncorneal-projecting neurons). Corneal-projecting neurons represented approximately 2% of all neuronal bodies (**Fig. 6B**). This fraction, along with noncorneal-projecting neurons as the control, was subjected to quantitative polymerase chain reaction (qPCR) analysis for the expression of nociceptors, neuropeptides, and neurotrophic factor receptors. The trigeminal ganglia of white light–exposed mice served as the control; there were no significant differences between isolated corneal-projecting neurons and noncorneal-projecting neurons, suggesting limited, if any, side effects of WGA labeling on the trigeminal ganglia. Blue light exposure upregulated TRPV1 in corneal-projecting neurons but not in the noncorneal-projecting neurons (**Fig. 6C**). On the other hand, TRPV4 expression is unchanged by blue light exposure, consistent with the results of our immunohistochemical studies shown in **Figure 5**. Interestingly, blue light exposure upregulated expression of SP (Tac1,Tachykinin Precursor 1), galanin (Gal), as well as TAFA Chemokine Like Family Member 1 (TAFA), and downregulated expression of calcitonin gene-related peptide (CGRP) in corneal-projecting neurons at 1 day after exposure. The receptors of neurotrophic factors, ciliary neurotrophic factor receptor subunit alpha (CNTFRα) and nerve growth factor receptor (NGFR), also increased in blue light–exposed corneal-projecting neurons, suggesting a potential tissue repair response at this time point.

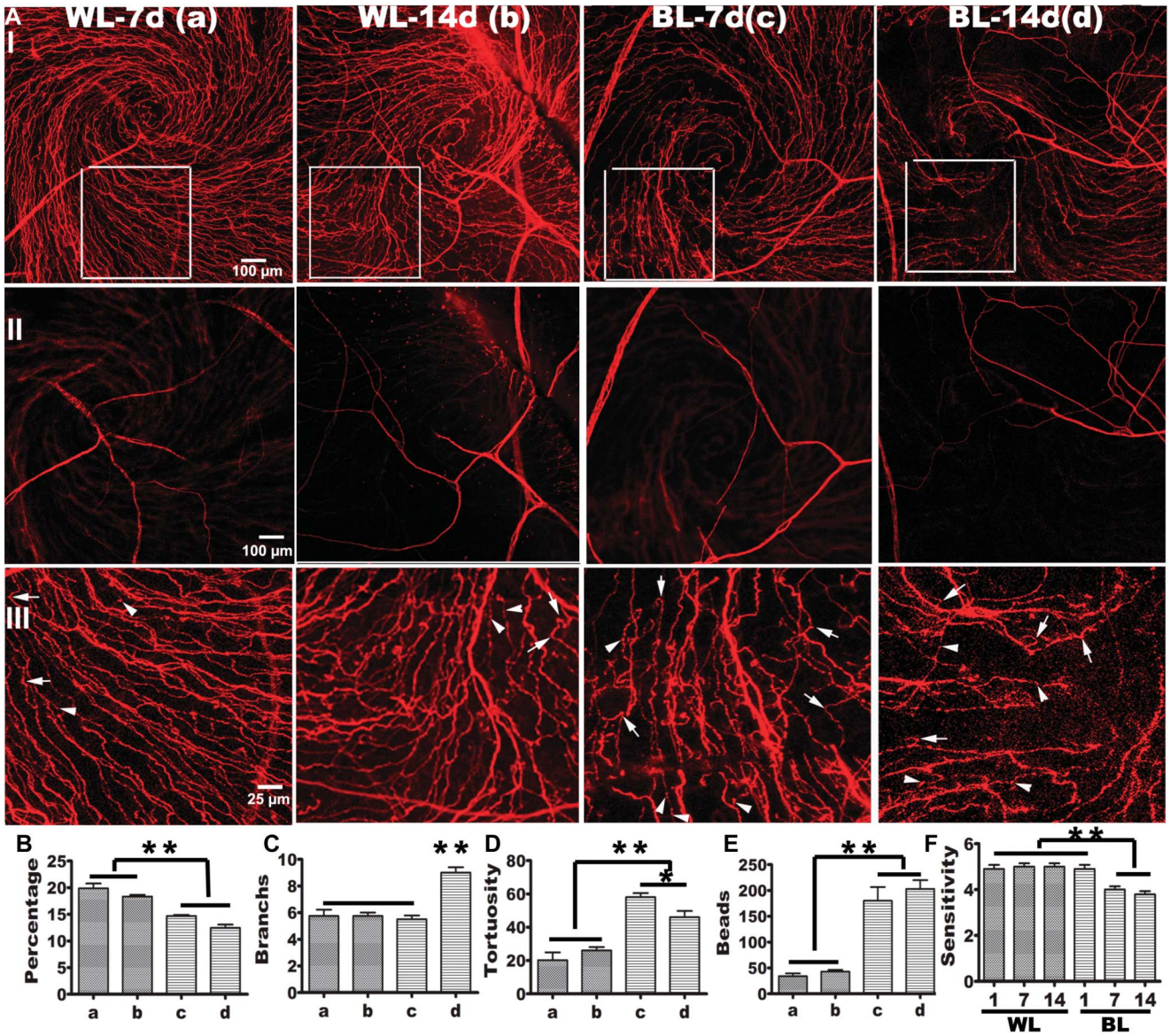

Figure 4. Corneal innervation and nerve structure in blue light–exposed mice. Corneas from white-light (WL) and blue-light (BL) exposed mice at the indicated times were collected and subjected to whole-mount confocal microscopy analysis with β-tubulin III. (I) Merged staining of the cornea at all optical layers. (II) Nerve branches at the stromal layer. (III) Intraepithelial nerve endings magnified from the marked area on A(I). Arrows: tortuous fibers, Arrowheads: bead-like formations (A). Corneal innervation was quantified as the percentage of threshold area positive for β-tubulin III staining (B). The number of branch points on the main nerve fibers per mm^2 (C), the number of the acute angle of fibers per mm^2 showing abrupt changes in direction (nerve tortuosity, D), and the number of beadlike structures present per mm^2 of nerve fiber (beadlike formations), (E) (**$P < 0.01$). (B–E) data were manually counted from images shown in A(III) and verified by a second blinded lab member (**$P < 0.05$, $P < 0.01$). Data of day 7 were from 3 corneas from female mice and day 14 from 4, 2 male and 2 female mice. Mice were subjected to cornea sensitivity measurements with an aesthesiometer (**$P < 0.01$, n = 10, 5 male and 5 female) (F).

3.6. Blue light exposure increases the density of SP^+ cells in the trigeminal ganglia and SP^+ sensory nerve fibers or endings in the cornea

To determine whether SP expression is upregulated at the protein level, we investigated the expression and distribution of SP in the trigeminal ganglion and cornea. **Figure 7A** shows that blue light induces a significant increase in the number of SP^+ corneal-projecting neurons at 3 days after exposure (p.e). Substance P seemed to be expressed in a selective group of $TRPV1^+$ corneal-projecting neurons in blue light–exposed trigeminal ganglia. Using whole-mount confocal microscopy, we further assessed whether upregulation of SP in the trigeminal ganglia also results in an upregulation in corneal nerve endings. At 3 days p.e., blue light–exposed corneas exhibited an increased number of SP^+ nerve endings compared with controls; at 5 days p.e., the density of SP^+ nerve endings was further increased in blue light–exposed corneas (**Figs. 7B and C**). At the protein levels, blue light exposure resulted in a significantly higher of SP expression when compared to white light in the corneas (Fig. 7D).

4. Discussion

In this study, we established an ocular neurological pain model in B6 mice using blue light exposure as a stressor. We found that blue light caused detectable decreases in tear secretion and increases in RB staining, but no fluorescein staining, suggesting that the epithelial barrier function remains relatively intact. An

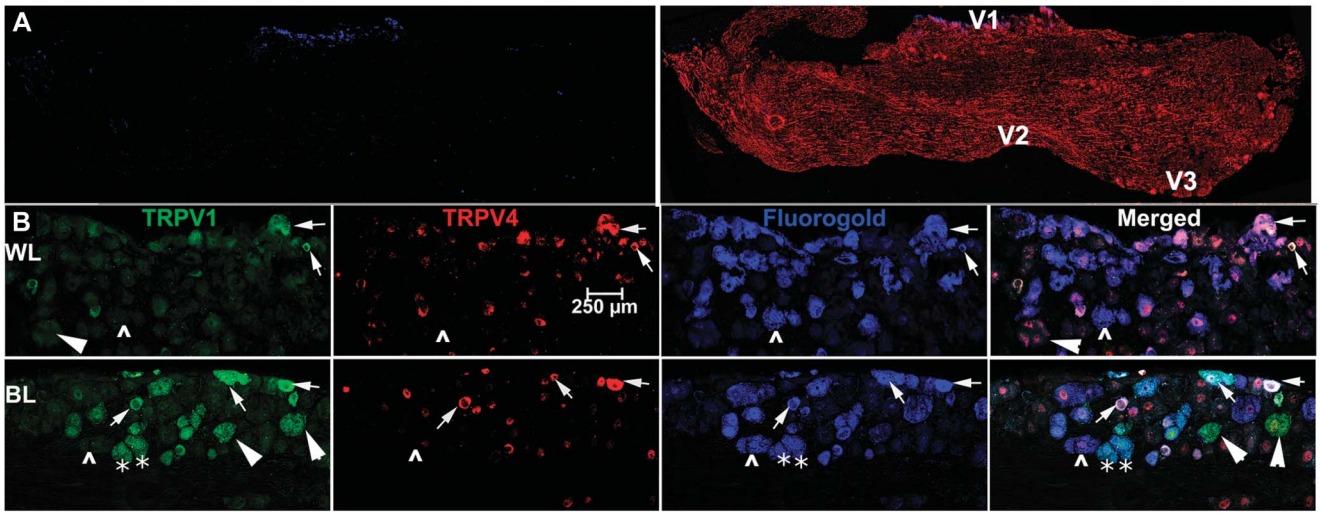

Figure 5. Colocalization and upregulation of TRPV1 with TRPV4 in corneal projecting neurons of blue light–exposed mice. 0.5 μL of FluoroGold was injected into the corneal stroma before light exposure. After 3 days exposure, trigeminal ganglia were cryostat sectioned and stained with β-tubulin III (A), TRPV1, and TRPV4 (B). The images were collected from the dorsomedial part of the trigeminal ganglion where retrograde-labeled corneal-projecting neurons are found. TRPV4$^+$ TRPV1$^+$ corneal-projecting neurons (arrows), TRPV1$^+$ TRPV4$^-$ (*) corneal-projecting neurons, TRPV1$^+$ TRPV4$^-$ FluoroGold$^-$ neurons (arrowhead), TRPV1$^+$ corneal-projecting neurons (^). Images represent one of at least 3 images from a representative experiment (from 2 independent experiments). BL, blue light; WL, white light.

increase in hypertonic or hypotonic solution–induced eye-wiping behaviors was also observed after 1 day of blue light exposure and is sustained up to day 14 in a trigeminal ganglion pain–dependent manner. However, increases in wind-induced eye closing and cold-induced blinking behaviors, 2 surrogate measures for assessing ocular hyperalgesia were detectable only after day 3. These further increased starting at 7 days p.e. and were maintained at elevated levels to day 14. Whole-mount confocal microscopy revealed that blue light exposure resulted in a decreased subbasal nerve plexus ending density, with increased stromal sensory branching, tortuosity, and beading. We also used stromal injection of FluoroGold for IHC staining and WGA for cell sorting of the trigeminal ganglia. We demonstrated that blue light exposure increased TRPV1 staining intensity, particularly in TRPV4$^+$ corneal-projecting neurons. It increased the expression of TRPV1, but not TRPV4, at the messenger RNA (mRNA) level in corneal-projecting neurons. Furthermore, blue light exposure increased the expressions of the neuropeptides Tac1 (encoding SP), galanin, and TAFA and decreased CGRP expression. There were more SP$^+$ corneal-projecting neurons in the trigeminal ganglia, with significantly more SP$^+$ nerve endings in the corneas of blue light–exposed mice (**Fig. 7**). Finally, blue light exposure also upregulated the expression of the neurotrophic factor receptors, CTNFRα and NGFR, suggesting a potential regenerative effort of injured corneal-projecting neurons in response to blue light stress. The results were summarized in **Table 1**. Taken together, we have established a murine model of human ocular neuropathic pain with multiple quantifiable parameters, and our results suggested that the upregulation of TRPV1 and SP may be contributing factors for the development of ocular pain.

We used an exposure protocol with a lower intensity of blue light at 2.72 mW/cm^2 (vs 6 mW/cm^2 for Marek et al.[36]) and longer exposure (12 hours each day, up to 14 days, vs 3 hours by Marek et al), yielding 117.6 J/cm^2 radiant exposure (vs 64.8 for Marek et al.). Among the nociceptive behaviors tested, changes in tear secretion and eye wiping were detected after 1 day of blue light exposure and remained at elevated levels for up to 14 days. Rapid alterations in tear secretion and stability in response to blue light exposure suggest a sensitive and tightly controlled sensory neuron circuit at the ocular surface, including the afferent sensory nerves in the cornea and conjunctiva and efferent parasympathetic and sympathetic nerves that innervate the lacrimal gland.[40] Decreased tear stability assessed by RB staining suggests involvement of the meibomian glands as well.[58] We showed that although exposure to both hyperosmolarity and hypoosmolarity, known to be performed by TRPV1[11] and TRPV4,[2] respectively, increased eye-wiping behaviors, the hyperosmolar exposure stimulated a much stronger response. The fact that corneal anesthesia significantly reduced hyperosmolarity stimulated eye wiping and abolished blue light–induced hyperalgesia suggests that the blue light exposure–induced increase in eye wiping is an outcome of corneal–trigeminal pain. How TRP channels transmit nociception signaling, leading to hyperalgesia, is currently under investigation in our laboratory.

An increase in wind-induced eye-closing and cold-induced eye-blinking behaviors was first detected at 3 days p.e. There was a second elevation starting at 7 days p.e., reaching peak levels at 9 days p.e., and remained elevated up to 14 days p.e. Strong winds may cause rapid evaporation of tears, a lowering of the ocular surface temperature, or increased tactile pressure, which nociceptors may detect. Cold, however, is detected by TRPM8 and TRPA.[38] In the cornea, TRPM8 is sensitized by TRPV1[29]; although in most cases, TRPV1 and TRPM8 are not expressed in the same C fibers.[52] The second peak in increased wind-induced eye closing and cold-induced eye blinking are likely due to further sensitization or further increases in the levels of TRPs, such as TRPV1 and TRPM8 in C fibers.[7,47,52] We speculate that these elevations in hyperalgesia may be responsible for converting acute to chronic ocular pain due to persistent light stress and sensory nerve injury.[61] Hence, our blue light–induced ocular pain model may also be a model for studying the transition between acute to chronic pain and how chronic pain is maintained and becomes autonomous regardless of stimuli.

Patients with ocular pain have varying degrees of reduced nerve fiber density, increased subbasal nerve tortuosity, nerve fiber beading, branching, and sprouting.[27,57] Our data show that blue light exposure resulted in sprouting from small nerve fibers (increase

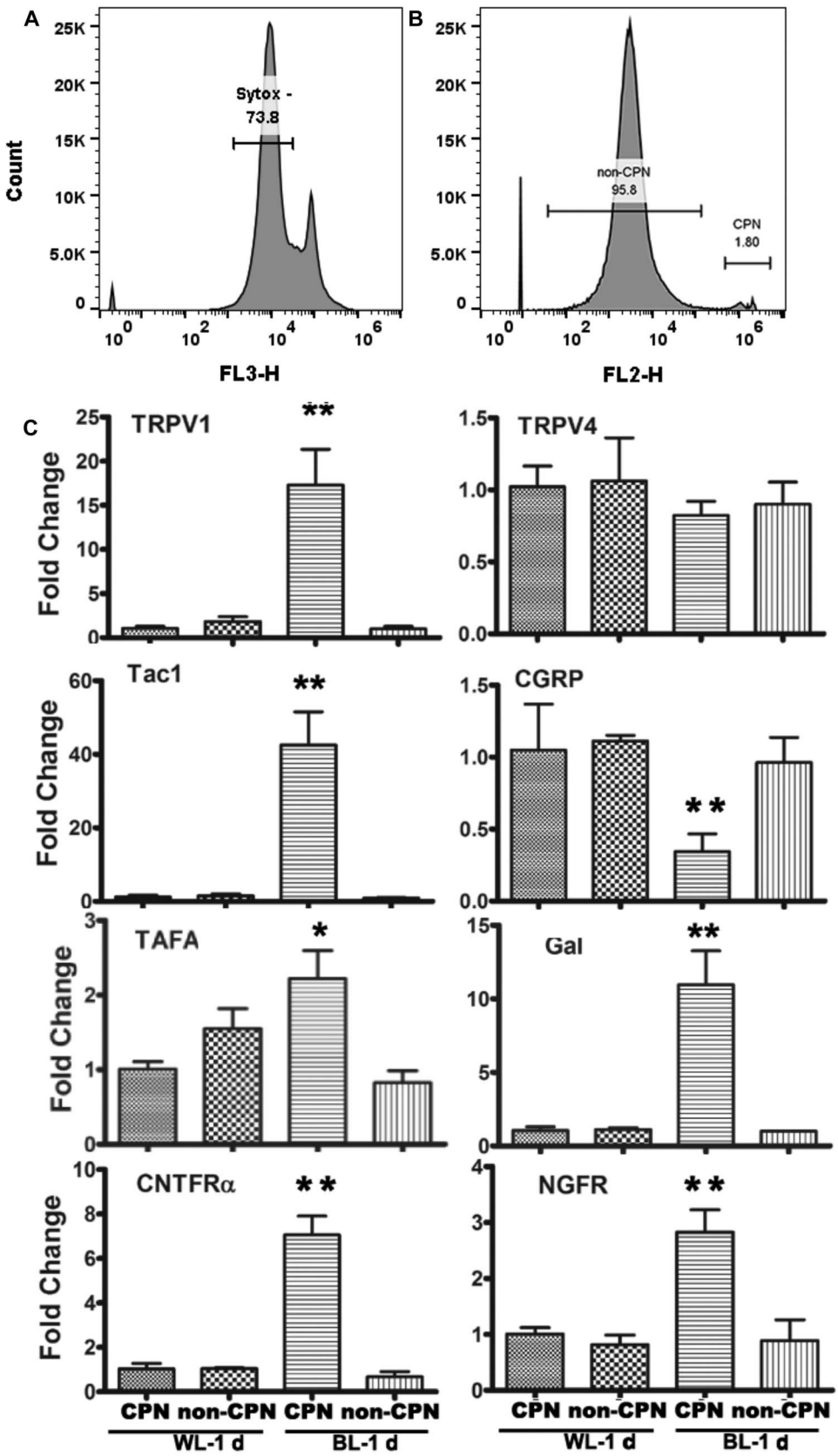

Figure 6. Altered expressions of TRPs and neuropeptide in corneal-projecting neurons of blue light–exposed mice. Corneal-projecting neurons were retrogradely labeled using wheat germ agglutinin–Alexa Fluor 555 (WGA). At 2 days postlabeling, the mice were exposed to cycles of either blue light (BL) or white light (WL) alternating with darkness. At 1 day after exposure, trigeminal ganglia were excised and digested. Neurons were isolated by Percoll density–gradient centrifugation and sorted by NanoCellect. Viable neuronal cells were identified using Sytox staining(A) WGA^+ $Sytox^-$ (corneal-projecting neurons) or WGA^- $Sytox^-$ neurons (noncorneal-projecting neurons) were sorted (B). Corneal-projecting neurons with noncorneal-projecting neurons cells as controls were subjected to qPCR analysis (C) (**$P < 0.01$, n = 3). CPN, corneal-projecting neuron.

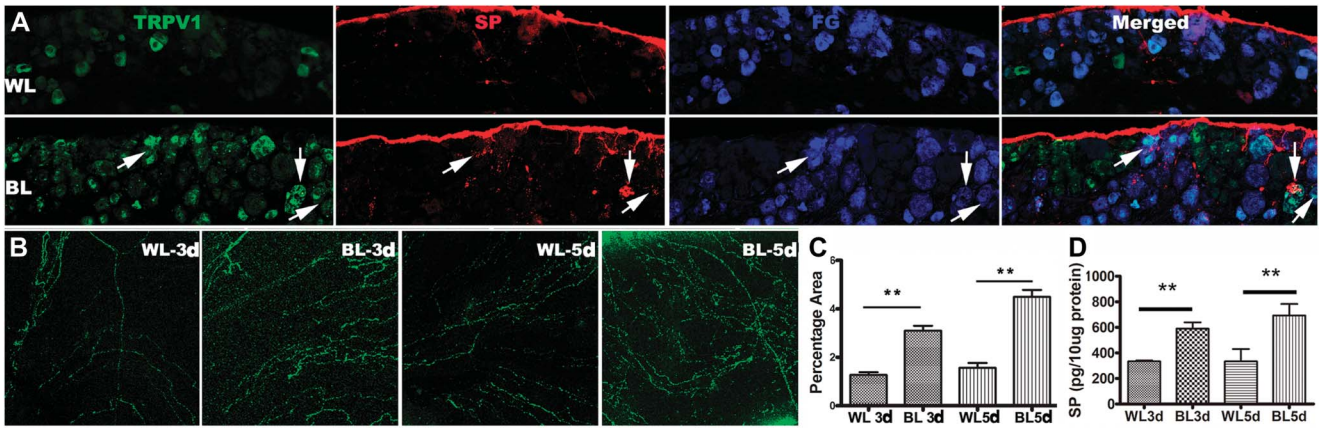

Figure 7. Substance P was released from TRPV1$^+$ corneal-projecting neurons. Corneal-projecting neurons were retrogradely labeled by FluoroGold and exposure with blue light (BL) or white light (WL). At 3 days after exposure, trigeminal ganglia were excised, cryostat sectioned, and stained for TRPV1 and SP. Arrows show SP expressed in TRPV1$^+$ corneal-projecting neurons (A). Corneas from white light and blue light–exposed mice at the indicated times were collected and subjected to whole-mount corneal confocal imaging analysis with SP staining (B). Images were quantified as the percentage of threshold area using Image J (C). (D) Measurement of SP in the corneas of control by ELISA, white light (WL 3 d and 5 d), and blue light (BL 3 d and BL 5 d) exposed mice. (**$P < 0.01$, n = 3). SP, substance P.

bead-like formations and nerve tortuosity) and nerve branching, with a significant decrease in sensory nerve density, similar to that observed in human patients with diabetes and ocular pain.[5,20] To compensate for blue light exposure–induced sensory nerve degeneration, regeneration must also occur. Indeed, we observed the upregulation of the receptors for neurotrophic factors NGF and CNTF in blue light exposed corneal-projecting neurons at 1 day post p.e. However, prolonged blue light exposure resulted in the dysregulation of axon degeneration and regeneration, and the presence of malformed sensory fibers and endings, as seen initially at 7 days p.e. and becoming more apparent at 14 day p.e. (**Fig. 4**). We conclude that blue light–induced hyperalgesia may be linked to structural abnormalities, which results in abnormal activation, firing, and pain transmission in a TRP channel–related manner. These altered corneal neuronal cytoarchitectures may also be the pathological basis for transforming ocular pain from the acute to chronic phase.

We used corneal stroma injections of FluoroGold for immunohistochemistry[33] and WGA for cell sorting. The FluoroGold-labeled cells are primarily located in the dorsal part of the ophthalmic region of the ipsilateral trigeminal ganglion (V1), consistent with the known location of the corneal-projecting neurons.[37] In control trigeminal ganglia, most, but not all, FluoroGold$^+$ cells were TRPV1$^+$ and are likely C-peptidergic neurons.[59] FluoroGold$^+$ TRPV1$^+$ cells are likely either Piezo2$^+$ C-tactile low-threshold mechanoreceptors[17] or Aδ fibers[22] in the trigeminal ganglion. TRPV4 staining colocalized with only a fraction of TRPV1$^+$ FluoroGold$^+$ neuron bundles, suggesting that TRPV4 was expressed in a limited number of C-peptidergic neurons. In blue light–exposed mice, staining intensity of TRPV1 was increased, and there were a few TRPV1 staining neurons that were FluoroGold$^-$, suggesting that corneal nerve injury induces TRPV1 expression in the corneal-projecting neurons and a few noncorneal-projecting neurons. This upregulation in noncorneal-projecting neurons may contribute to sensitization and hyperalgesia, as suggested by Tran et al.[60] How blue light–induced injury causes noncorneal-projecting neurons in the trigeminal ganglia to express TRPV1 is of great interest in understanding ocular pain. We propose that this is due to the release of neuropeptides from neighboring corneal-projecting neurons. Indeed, we detected the upregulation of neuropeptides SP, galanin, and TAFA in the corneal-projecting neuron of blue light–exposed mice using cell sorting and qPCR.

Retrograde labeling and cell sorting with WGA revealed that 2% of trigeminal ganglia were corneal-projecting neurons. Our study, for the first time, showed that the expression of neuropeptides, Tac1, galanin, and TAFA were upregulated, whereas CGRP was downregulated in corneal-projecting neurons in blue light–exposed mice after 1 day. The upregulation of SP was confirmed in the trigeminal ganglia and cornea. Significantly more SP$^+$ sensory nerve endings

Table 1

Summary of nociception and structural molecular alterations in blue light exposure. ND: no detection)

Days	Behavior changes	Tear film abnormalities	Structural changes (corneal innervation)	Molecular changes
1	Eye wiping ↑	Tear secretion↑ Rose Bengal staining↑	ND	TRPV1↑,Tac1↑,Gal1↑, CGRP↓
3	Eye wiping↑ Blinking or closing↑	Tear secretion↑ Rose Bengal staining↑	ND	TRPV1↑
7	Eye wiping↑ Blinking or closing↑	Tear secretion↑ Rose Bengal staining↑	Altered	ND
9	Eye wiping↑ Blinking or closing↑	Tear secretion↑ Rose Bengal staining↑	ND	ND
14	Eye wiping↑ Blinking or closing↑	Tear secretion↑ Rose Bengal staining↑	Altered	ND

were found in the cornea of blue light–exposed mice after day 3. This increase is more pronounced after day 5. The increase in SP^+ sensory nerve endings may be associated with wind-induced and cold-induced ocular hyperalgesia and the transformation of acute to chronic pain, as shown by Li et al.[29] On the other hand, the downregulation of CGRP is intriguing as elevated expression of CGRP in the trigeminal system is associated with migraine.[15] One potential explanation is that the expression of CGRP is time dependent. Unlike CGRP and SP, the roles of galanin and TAFA in nociception and ocular pain are less clear. Further studies are warranted to understand the role of different neuropeptides and nociceptors in the initialization and maintenance of ocular neuropathic pain.

In humans, females have a higher incidence rate and severe pain, many of which are related to dry eye diseases.[13,34] In this study, we did not see detectable sex differences in tearing, hyperalgesia responses, and structural alteration of sensory nerves in response to blue light exposure. In humans, ocular pain may be driven by dry eye disease; whereas in our animal model, the damage of the sensory nerve is caused by continuous exposure to blue light. Furthermore, aging is a known risk factor for dry eye and ocular pain, particularly for women, while the mice we used were relatively young. Nevertheless, our inability to reproduce these gender-specific differences is a limitation of our animal model.

In conclusion, in addition to dry eye and corneal sensation, blue light exposure leads to measurable ocular hyperalgesia, as well as upregulation of TRPV1, SP, galanin, TAFA in the trigeminal ganglia, and increased SP expression in the corneas of blue light–exposed mice. The blue light exposure model is suitable for assessing the mechanisms underlying the pathogenesis of ocular neuropathic pain and the transformation of ocular pain from acute to chronic states.

Conflict of interest statement

The authors have no conflict of interest to declare.

Acknowledgments

Supported by the National Institutes of Health, National Eye Institute (NEI) (R01EY10869 and EY17960 to F.-s. X. Yu), p30 EY004068 (NEI Core to Wayne State University), and Research to Prevent Blindness (to Kresge Eye Institute).

Supplemental digital content

Supplemental digital content associated with this article can be found online at http://links.lww.com/PAIN/B805.

Supplemental video content

A video abstract associated with this article can be found on the *PAIN* website.

Article history:
Received 28 November 2022
Received in revised form 23 January 2023
Accepted 3 February 2023
Available online 21 April 2023

References

[1] Alamri A, Bron R, Brock JA, Ivanusic JJ. Transient receptor potential cation channel subfamily V member 1 expressing corneal sensory neurons can be subdivided into at least three subpopulations. Front Neuroanat 2015;9:71.
[2] Alessandri-Haber N, Yeh JJ, Boyd AE, Parada CA, Chen X, Reichling DB, Levine JD. Hypotonicity induces TRPV4-mediated nociception in rat. Neuron 2003;39:497–511.
[3] Algvere PV, Marshall J, Seregard S. Age-related maculopathy and the impact of blue light hazard. Acta Ophthalmol Scand 2006;84:4–15.
[4] Barabino S, Shen L, Chen L, Rashid S, Rolando M, Dana MR. The controlled-environment chamber: a new mouse model of dry eye. Invest Opthalmol Vis Sci 2005;46:2766–71.
[5] Belmonte C, Aracil A, Acosta MC, Luna C, Gallar J. Nerves and sensations from the eye surface. Ocul Surf 2004;2:248–53.
[6] Belmonte C, Nichols JJ, Cox SM, Brock JA, Begley CG, Bereiter DA, Dartt DA, Galor A, Hamrah P, Ivanusic JJ, Jacobs DS, McNamara NA, Rosenblatt MI, Stapleton F, Wolffsohn JS. TFOS DEWS II pain and sensation report. Ocul Surf 2017;15:404–37.
[7] Bereiter DA, Rahman M, Thompson R, Stephenson P, Saito H. TRPV1 and TRPM8 channels and nocifensive behavior in a rat model for dry eye. Invest Ophthalmol Vis Sci 2018;59:3739–46.
[8] Bian F, Xiao Y, Zaheer M, Volpe EA, Pflugfelder SC, Li DQ, de Paiva CS. Inhibition of NLRP3 inflammasome pathway by Butyrate improves corneal wound healing in corneal alkali burn. Int J Mol Sci 2017;18:562.
[9] Chawla A, Lim TC, Shikhare SN, Munk PL, Peh WCG. Computer vision syndrome: darkness under the shadow of light. Can Assoc Radiol J 2019;70:5–9.
[10] Cho J, Bell N, Botzet G, Vora P, Fowler BJ, Donahue R, Bush H, Taylor BK, Albuquerque RJC. Latent sensitization in a mouse model of ocular neuropathic pain. Transl Vis Sci Technol 2019;8:6.
[11] Ciura S, Liedtke W, Bourque CW. Hypertonicity sensing in organum vasculosum lamina terminalis neurons: a mechanical process involving TRPV1 but not TRPV4. J Neurosci 2011;31:14669–76.
[12] Colloca L, Ludman T, Bouhassira D, Baron R, Dickenson AH, Yarnitsky D, Freeman R, Truini A, Attal N, Finnerup NB, Eccleston C, Kalso E, Bennett DL, Dworkin RH, Raja SN. Neuropathic pain. Nat Rev Dis Primers 2017;3:17002.
[13] Dance A. Why the sexes don't feel pain the same way. Nature 2019;567:448–50.
[14] Duerr ER, Chang A, Venkateswaran N, Goldhardt R, Levitt RC, Gregori NZ, Sarantopoulos CD, Galor A. Resolution of pain with periocular injections in a patient with a 7-year history of chronic ocular pain. Am J Ophthalmol Case Rep 2019;14:35–8.
[15] Edvinsson L. Role of CGRP in migraine. Handb Exp Pharmacol 2019;255:121–30.
[16] Farazifard R, Safarpour F, Sheibani V, Javan M. Eye-wiping test: a sensitive animal model for acute trigeminal pain studies. Brain Res Protoc 2005;16:44–9.
[17] Fernandez-Trillo J, Florez-Paz D, Inigo-Portugues A, Gonzalez-Gonzalez O, Del Campo AG, Gonzalez A, Viana F, Belmonte C, Gomis A. Piezo2 mediates low-threshold mechanically evoked pain in the cornea. J Neurosci 2020;40:8976–93.
[18] Galor A, Batawi H, Felix ER, Margolis TP, Sarantopoulos KD, Martin ER, Levitt RC. Incomplete response to artificial tears is associated with features of neuropathic ocular pain. Br J Ophthalmol 2016;100:745–9.
[19] Gao N, Yan C, Lee P, Sun H, Yu FS. Dendritic cell dysfunction and diabetic sensory neuropathy in the cornea. J Clin Invest 2016;126:1998–2011.
[20] Goyal S, Hamrah P. Understanding neuropathic corneal pain—gaps and current therapeutic approaches. Semin Ophthalmol 2016;31:59–70.
[21] Guarino BD, Paruchuri S, Thodeti CK. The role of TRPV4 channels in ocular function and pathologies. Exp Eye Res 2020;201:108257.
[22] Guerrero-Moreno A, Baudouin C, Melik Parsadaniantz S, Reaux-Le Goazigo A. Morphological and functional changes of corneal nerves and their contribution to peripheral and central sensory abnormalities. Front Cell Neurosci 2020;14:610342.
[23] Heaton JT, Kowaleski J, Edwards C, Smitson C, Hadlock TA. Evidence for facial nerve-independent mechanisms of blinking in the rat. Invest Opthalmol Vis Sci 2010;51:179–82.
[24] Hegarty DM, Hermes SM, Morgan MM, Aicher SA. Acute hyperalgesia and delayed dry eye after corneal abrasion injury. Pain Rep 2018;3:e664.
[25] Hirata H, Oshinsky ML. Ocular dryness excites two classes of corneal afferent neurons implicated in basal tearing in rats: involvement of transient receptor potential channels. J Neurophysiol 2012;107:1199–209.
[26] Jiao H, Ivanusic JJ, McMenamin PG, Chinnery HR. Distribution of corneal TRPV1 and its association with immune cells during homeostasis and injury. Invest Ophthalmol Vis Sci 2021;62:6.
[27] Labbe A, Alalwani H, Van Went C, Brasnu E, Georgescu D, Baudouin C. The relationship between subbasal nerve morphology and corneal sensation in ocular surface disease. Invest Opthalmol Vis Sci 2012;53:4926–31.

[28] Launay PS, Godefroy D, Khabou H, Rostene W, Sahel JA, Baudouin C, Melik Parsadaniantz S, Reaux-Le Goazigo A. Combined 3DISCO clearing method, retrograde tracer and ultramicroscopy to map corneal neurons in a whole adult mouse trigeminal ganglion. Exp Eye Res 2015;139: 136–43.

[29] Li F, Yang W, Jiang H, Guo C, Huang AJW, Hu H, Liu Q. TRPV1 activity and substance P release are required for corneal cold nociception. Nat Commun 2019;10:5678.

[30] Lin JB, Gerratt BW, Bassi CJ, Apte RS. Short-wavelength light-blocking eyeglasses attenuate symptoms of eye fatigue. Invest Ophthalmol Vis Sci 2017;58:442–7.

[31] Lin Z, Liu X, Zhou T, Wang Y, Bai L, He H, Liu Z. A mouse dry eye model induced by topical administration of benzalkonium chloride. Mol Vis 2011; 17:257–64.

[32] Loh K, Redd S. Understanding and preventing computer vision syndrome. Malays Fam Phys 2008;3:128–30.

[33] Lopez de Armentia M, Cabanes C, Belmonte C. Electrophysiological properties of identified trigeminal ganglion neurons innervating the cornea of the mouse. Neuroscience 2000;101:1109–15.

[34] Ma M, Yuan Q, Ye L, Liu K, Ye L, Min YL, Jiang N, Li Q, Shi W, Xu X, Zhu P, Shao Y. An experimental study of amniotic lacrimal duct stents in the treatment of perimenopausal female rabbits with dry eye. Mol Med Rep 2019;19:1056–64.

[35] Malin SA, Davis BM, Molliver DC. Production of dissociated sensory neuron cultures and considerations for their use in studying neuronal function and plasticity. Nat Protoc 2007;2:152–60.

[36] Marek V, Reboussin E, Degardin-Chicaud J, Charbonnier A, Dominguez-Lopez A, Villette T, Denoyer A, Baudouin C, Reaux-Le Goazigo A, Melik Parsadaniantz S. Implication of melanopsin and trigeminal neural pathways in blue light photosensitivity in vivo. Front Neurosci 2019;13: 497.

[37] Marfurt CF, Del Toro DR. Corneal sensory pathway in the rat: a horseradish peroxidase tracing study. J Comp Neurol 1987;261:450–9.

[38] McKemy DD. How cold is it? TRPM8 and TRPA1 in the molecular logic of cold sensation. Mol Pain 2005;1:16.

[39] Mecum NE, Demers D, Sullivan CE, Denis TE, Kalliel JR, Meng ID. Lacrimal gland excision in male and female mice causes ocular pain and anxiety-like behaviors. Sci Rep 2020;10:17225.

[40] Meng ID, Kurose M. The role of corneal afferent neurons in regulating tears under normal and dry eye conditions. Exp Eye Res 2013;117: 79–87.

[41] Messlinger K, Balcziak LK, Russo AF. Cross-talk signaling in the trigeminal ganglion: role of neuropeptides and other mediators. J Neural Transm (Vienna) 2020;127:431–44.

[42] Midena E, Brugin E, Ghirlando A, Sommavilla M, Avogaro A. Corneal diabetic neuropathy: a confocal microscopy study. J Refract Surg 2006; 22:S1047–52.

[43] Moein HR, Akhlaq A, Dieckmann G, Abbouda A, Pondelis N, Salem Z, Muller RT, Cruzat A, Cavalcanti BM, Jamali A, Hamrah P. Visualization of microneuromas by using in vivo confocal microscopy: an objective biomarker for the diagnosis of neuropathic corneal pain? Ocul Surf 2020; 18:651–6.

[44] Mowatt L, Gordon C, Santosh ABR, Jones T. Computer vision syndrome and ergonomic practices among undergraduate university students. Int J Clin Pract 2018;72:e13035.

[45] Niwano Y, Iwasawa A, Tsubota K, Ayaki M, Negishi K. Protective effects of blue light-blocking shades on phototoxicity in human ocular surface cells. BMJ Open Ophthalmol 2019;4:e000217.

[46] Okada Y, Sumioka T, Ichikawa K, Sano H, Nambu A, Kobayashi K, Uchida K, Suzuki Y, Tominaga M, Reinach PS, Hirai SI, Jester JV, Miyajima M, Shirai K, Iwanishi H, Kao WWY, Liu CY, Saika S. Sensory nerve supports epithelial stem cell function in healing of corneal epithelium in mice: the role of trigeminal nerve transient receptor potential vanilloid 4. Lab Invest 2019;99:210–30.

[47] Pabbidi MR, Premkumar LS. Role of transient receptor potential channels Trpv1 and Trpm8 in diabetic peripheral neuropathy. J Diabetes Treat 2017;2017:029.

[48] Pina R, Ugarte G, Campos M, Inigo-Portugues A, Olivares E, Orio P, Belmonte C, Bacigalupo J, Madrid R. Role of TRPM8 channels in altered cold sensitivity of corneal primary sensory neurons induced by axonal damage. J Neurosci 2019;39:8177–92.

[49] Puja G, Sonkodi B, Bardoni R. Mechanisms of peripheral and central pain sensitization: focus on ocular pain. Front Pharmacol 2021;12:764396.

[50] Rosenfield M. Computer vision syndrome: a review of ocular causes and potential treatments. Ophthalmic Physiol Opt 2011;31:502–15.

[51] Sanchez-Valerio MDR, Mohamed-Noriega K, Zamora-Ginez I, Baez Duarte BG, Vallejo-Ruiz V. Dry eye disease association with computer exposure time among subjects with computer vision syndrome. Clin Ophthalmol 2020;14:4311–7.

[52] Schecterson LC, Pazevic AA, Yang R, Matulef K, Gordon SE. TRPV1, TRPA1, and TRPM8 are expressed in axon terminals in the cornea: TRPV1 axons contain CGRP and secretogranin II; TRPA1 axons contain secretogranin 3. Mol Vis 2020;26:576–87.

[53] Sheppard AL, Wolffsohn JS. Digital eye strain: prevalence, measurement and amelioration. BMJ Open Ophthalmol 2018;3:e000146.

[54] Stevenson W, Chen Y, Lee SM, Lee HS, Hua J, Dohlman T, Shiang T, Dana R. Extraorbital lacrimal gland excision: a reproducible model of severe aqueous tear-deficient dry eye disease. Cornea 2014;33:1336–41.

[55] Tashiro A, Okamoto K, Chang Z, Bereiter DA. Behavioral and neurophysiological correlates of nociception in an animal model of photokeratitis. Neuroscience 2010;169:455–62.

[56] Taylor HR, Munoz B, West S, Bressler NM, Bressler SB, Rosenthal FS. Visible light and risk of age-related macular degeneration. Trans Am Ophthalmol Soc 1990;88:163–73. discussion 173–8.

[57] Tervo TM, Moilanen JAO, Rosenberg ME, Tuominen ISJ, Valle T, Vesaluoma MH. In vivo confocal microscopy for studying corneal diseases and conditions associated with corneal nerve damage. Adv Exp Med Biol 2002;506:657–65.

[58] Tomlinson A, Bron AJ, Korb DR, Amano S, Paugh JR, Pearce EI, Yee R, Yokoi N, Arita R, Dogru M. The international workshop on meibomian gland dysfunction: report of the diagnosis subcommittee. Invest Ophthalmol Vis Sci 2011;52:2006–49.

[59] Tracey WD Jr. Nociception. Curr Biol 2017;27:R129–33.

[60] Tran EL, Crawford LK. Revisiting PNS plasticity: how uninjured sensory afferents promote neuropathic pain. Front Cell Neurosci 2020;14: 612982.

[61] Voscopoulos C, Lema M. When does acute pain become chronic? Br J Anaesth 2010;105(suppl 1):i69–85.

[62] Wang F, Gao N, Yin J, Yu FSX. Reduced innervation and delayed re-innervation after epithelial wounding in type 2 diabetic Goto-Kakizaki rats. Am J Pathol 2012;181:2058–66.

[63] Wenk NH, Honda NC. Silver nitrate cauterization: characterization of a new model of corneal inflammation and hyperalgesia in rat. PAIN 2003; 105:393–401.

[64] Yan ZX, Luo Y, Liu NF. Blockade of angiopoietin-2/Tie2 signaling pathway specifically promotes inflammation-induced angiogenesis in mouse cornea. Int J Ophthalmol 2017;10:1187–94.

[65] Yin J, Huang J, Chen C, Gao N, Wang F, Yu FSX. Corneal complications in streptozocin-induced type I diabetic rats. Invest Ophthalmol Vis Sci 2011;52:6589–96.